Correlation of Scar in Cardiac MRI and High-Resolution Contact Mapping of Left Ventricle in a Chronic Infarct Model

ANEES THAJUDEEN, M.D.,* WARREN M. JACKMAN, M.D.,† BRIAN STEWART, M.S.,‡ IVAN COKIC, M.D.,§ HIROSHI NAKAGAWA, M.D., PH.D.,† MICHAEL SHEHATA, M.D.,* ALLEN M. AMORN, M.D.,* AVINASH KALI, M.S.,§,¶ EZH LIU, M.D.,* DORON HARLEV, M.SC.,‡ NATHAN BENNETT, M.ENG.,‡ ROHAN DHARMAKUMAR, PH.D.,§,¶ SUMEET S. CHUGH, M.D.,*,** and XUNZHANG WANG, M.D.*

From the *Heart Institute and §Biomedical Imaging Research Institute, Cedars Sinai Medical Center, Los Angeles, California; †Heart Rhythm Institute, University of Oklahoma, Oklahoma City, Oklahoma; ‡Rhythmia Medical, Boston Scientific, Marlborough, Massachusetts; ¶Department of Bioengineering, University of California, Los Angeles, California; and **David Geffen School of Medicine, University of California, Los Angeles, California

Background: *Endocardial mapping for scars and abnormal electrograms forms the most essential component of ventricular tachycardia ablation. The utility of ultra-high resolution mapping of ventricular scar was assessed using a multielectrode contact mapping system in a chronic canine infarct model.*

Methods: *Chronic infarcts were created in five anesthetized dogs by ligating the left anterior descending coronary artery. Late gadolinium-enhanced magnetic resonance imaging (LGE MRI) was obtained 4.9 ± 0.9 months after infarction, with three-dimensional (3D) gadolinium enhancement signal intensity maps at 1-mm and 5-mm depths from the endocardium. Ultra-high resolution electroanatomical maps were created using a novel mapping system (Rhythmia Mapping System, Rhythmia Medical/Boston Scientific, Marlborough, MA, USA) Rhythmia Medical, Boston Scientific, Marlborough, MA, USA with an 8.5F catheter with mini-basket electrode array (64 tiny electrodes, 2.5-mm spacing, center-to-center).*

Results: *The maps contained 7,754 ± 1,960 electrograms per animal with a mean resolution of 2.8 ± 0.6 mm. Low bipolar voltage (<2 mV) correlated closely with scar on the LGE MRI and the 3D signal intensity map (1-mm depth). The scar areas between the MRI signal intensity map and electroanatomic map matched at 87.7% of sites. Bipolar and unipolar voltages, compared in 592 electrograms from four MRI-defined scar types (endocardial scar, epicardial scar, mottled transmural scar, and dense transmural scar) as well as normal tissue, were significantly different. A unipolar voltage of <13 mV correlated with transmural extension of scar in MRI. Electrograms exhibiting isolated late potentials (ILPs) were manually annotated and ILP maps were created showing ILP location and timing. ILPs were identified in 203 ± 159 electrograms per dog (within low-voltage areas) and ILP maps showed gradation in timing of ILPs at different locations in the scar.*

This work was supported in part by a grant from the National Heart, Lung, and Blood Institute (R01 HL-091989) and by Rhythmia Medical, MA, USA.

Disclosures: Anees Thajudeen, Ivan Cokic, Michael Shehata, Avinash Kali, Allen Amorn, Ezh Liu, Rohan Dharmakumar, Sumeet S. Chugh, and Xunzhang Wang report no conflicts of interest or relevant disclosures. Drs. Warren Jackman and Hiroshi Nakagawa are consultants for Boston Scientific and were consultants and shareholders in Rhythmia Medical, which was subsequently acquired by Boston Scientific. Brian Stewart, Nathan Bennet, and Doron Harlev receive salary from and have equity interests in Boston Scientific. Doron Harlev and Brian Stewart also hold patents related to the Rhythmia mapping system.

Address for reprints: Warren M. Jackman, M.D., Heart Rhythm Institute, University of Oklahoma Health Sciences Center, 1200 Everett Drive, Rm 6E-103, Oklahoma City, OK 73104. Fax: 405-271-9696; e-mail: warren-jackman@ouhsc.edu

Received August 15, 2014; revised November 27, 2014; accepted December 16, 2014.

doi: 10.1111/pace.12581

Conclusions: *Ultra-high resolution contact electroanatomical mapping accurately localizes ventricular scar and abnormal myocardial tissue in this chronic canine infarct model. The high fidelity electrograms provided clear identification of the very low amplitude ILPs within the scar tissue and has the potential to quickly identify targets for ablation. (PACE 2015; 38:663–674)*

ventricular tachycardia, electroanatomical mapping, magnetic resonance imaging, late potentials, ventricular scar

Introduction

Catheter ablation of ventricular tachycardia (VT) in patients with prior myocardial infarction is frequently limited by the presence of multiple inducible VTs. Activation mapping is not possible for the majority of the tachycardias (unmappable), either because of hemodynamic instability during the tachycardia or because the tachycardia is not sustained, not reinducible, or changes to another tachycardia before mapping can be completed.[1] The substrate for the multiple reentrant circuits is the interconnecting network of surviving myocardial bundles within the scar.[2] Substrate mapping to identify the abnormal low-voltage areas and the critical components of possible VT circuits (surviving myocardial bundles) is an effective strategy and often the only method available. Although several approaches have been utilized for substrate mapping,[3–6] one of the simplest and most direct is to record the isolated late potentials (ILPs) generated by the late activation of the isolated myocardial bundles during sinus rhythm[5,7–9] or ventricular pacing. This approach has two limitations. Ablation success often requires recording with very high density throughout the scar (every 2–3 mm) to target all accessible ILPs (all possible circuits). This density is difficult to achieve using point-by-point mapping with a conventional ablation catheter. Further, the ILPs are very small, with a bipolar voltage <0.1 mV. These low-amplitude signals are difficult to identify unless noise levels are reduced.

The purpose of this study is to test a new high resolution, contact mapping system in a chronic canine infarct model to delineate scar geometry, and to identify the location of ILPs within chronic infarct scar. The multielectrode catheter and the integrated mapping system (Rhythmia Medical/Boston Scientific, Marlborough, MA, USA) has been previously studied for high-density contact mapping in canine right atrium and normal porcine left ventricle where it demonstrated high mapping accuracy (for activation mapping) and significantly reduced mapping time.[10,11] In this study, we compared the activation and voltage maps in infarcted canine hearts with late gadolinium-enhanced magnetic resonance imaging (LGE MRI) information. We tested the hypotheses that low amplitude, closely spaced bipolar electrograms accurately localize the endocardial component of the infarct scar and that the unipolar electrogram amplitude may correlate with the thickness of the scar. The utility of the high-resolution mapping system to accurately identify ILPs was ascertained.

Methods

The Experimental Preparation

Five mongrel dogs weighing 20–25 kg were used for the chronic infarct model.[9,12,13] The protocol was approved by the Institutional Animal Care and Use Committee at Cedars-Sinai Medical Center, Los Angeles, CA, USA. After pretreatment with amiodarone (200 mg/day) for 7 days, the dogs were anesthetized with propofol (5.0–7.5 mg/kg i.v.), endotracheally intubated, and maintained on gas anesthesia (2.0–2.5% isoflurane with 100% oxygen). A left thoracotomy was performed through the fourth intercostal space and the left anterior descending (LAD) coronary artery was ligated prior to the first diagonal branch. The dogs were recovered and treated with analgesics and antibiotics. Amiodarone was discontinued after surgical ligation. The animals survived the thoracotomy without significant arrhythmia or other adverse event.

Cardiac MRI

Animals underwent cardiac MRI on day 7 (acute) and at month 4–6 (chronic) following LAD ligation. Cardiac magnetic resonance studies were performed on a clinical 3.0T MRI system (MAGNETOM Verio, Siemens Medical Solutions, Erlangen, Germany) equipped with a high-performance gradient system (maximum gradient amplitude of 45 mT/m and maximum slew rate of 200 T/m/s). The animals were anesthetized, intubated, and ventilated as described above for the LAD ligation procedure. Cardiac gating was achieved by using electrocardiogram (ECG) triggering and breath-holding was achieved by suspending ventilation at end-expiration. For LGE MRI imaging, gadolinium-DTPA (0.2 mmol/kg of body wt., OptiMARK, Mallinckrodt Inc., Hazelwood, MO, USA) was administered intravenously using a power injector followed by a 20-mL saline flush. An optimal inversion time (TI)

to null the apparent normal myocardium was then determined from TI scout images. LGE MRI images were acquired 10–15 minutes after contrast administration. Multiple cardiac-gated breath-held two-dimensional (2D) images of contiguous short-axis sections (6-mm sections) covering the entire left ventricular (LV) and the three long-axis views (two chamber, three chamber, and four chamber) were acquired using an inversion recovery prepared FLASH (TR/TE = 3.0/1.5 ms, flip angle = 25° BW = 586 Hz/pixel and slice thickness = 6 mm) sequence at mid-diastole.

The gray scale LGE MRI images (2D slices), with voxel size of 1 mm^3, were analyzed and five different tissue types were defined based on the pattern of enhancement.[14] The enhancement was categorized by the number of standard deviations (SD) above the mean intensity of a remote area of normal tissue on each slice (baseline intensity). These five tissue types are:

1. Normal tissue: Areas with gadolinium enhancement intensity less than three SD above baseline intensity in remote normal myocardium.
2. Transmural dense scar: Tissue with uninterrupted gadolinium enhancement intensity greater than five SD above baseline that extends from endocardium to epicardium.
3. Transmural mottled scar: Tissue with gadolinium enhancement intensity greater than three SD above baseline, from endocardium to epicardium, with some tissue of intensity more than five SD above baseline.
4. Endocardial scar: Layer of tissue with signal intensity more than five SD above baseline at the endocardium, with normal tissue between the scar and epicardial surface.
5. Epicardial scar: Layer of tissue with signal intensity more than five SD at the epicardium, with normal tissue between the scar and the blood pool.

MRI Signal Intensity Maps

To localize and measure infarct scar, color maps indicating magnetic resonance (MR) signal intensity were created at various myocardial depths. This was accomplished by first manually segmenting the blood pool using both LGE and T2 MR images and then constructing a three-dimensional (3D) surface that encloses that segmented blood pool. This process produced an endocardial surface from the MR data. This surface was expanded toward the epicardium in nine steps of 1 mm each to create 10 surfaces (3D shells) that pass through the myocardium at various equally spaced tissue depths away from the endocardial surface. Each point in this surface was given an LGE MR intensity value by interpolating the LGE MR voxel (voxel size 1 mm^3) values at the appropriate coordinates. MATLAB (MathWorks, Natick, MA, USA), OsiriX (Pixmeo, Geneva, Switzerland), and the Rhythmia Mapping System (Boston Scientific) software were used for the above process.

Endocardial scar measurements were made using the 1-mm myocardial depth (blood pool expanded outward by 1 mm into the tissue). Epicardial scar measurements were made using the 5-mm myocardial depth. A 5-mm depth was chosen for the epicardial scar because in areas of transmural infarction, the myocardial depth varied from 5 mm to 10 mm, as is also evident from previous animal infarct studies.[13] The resulting 3D signal intensity maps are referred to as the endocardial and epicardial LGE maps. The color scale in the LGE maps correspond to the signal intensity of the voxels in the actual cardiac MRI slices.

Electroanatomical Mapping

Electrophysiological study and LV endocardial mapping was performed 4.9 ± 0.9 months after infarction and within 2 weeks of capturing the chronic cardiac MRI. Under general anesthesia, multielectrode catheters were inserted into the coronary sinus and right ventricle. LV mapping was performed during sinus rhythm using a novel 64 electrode mini-basket catheter (IntellaMap Orion Mapping Catheter, Boston Scientific) and mapping system (Rhythmia Mapping System). The details of the mapping system have been described previously.[10] The 8.5F bidirectional catheter has a mini-basket electrode array containing eight splines, each with eight tiny electrodes (area 0.4 mm^2 and 2.5 mm spacing, center-to-center, Fig. 1). The basket can be deployed to varying diameter (minimum 3 mm, nominal 18 mm, and maximum 22 mm). The location of each electrode is determined using a combination of magnetic sensor located at the tip of the catheter and impedance sensing at each of the electrodes. The mapping system software is run on a computer workstation and has an electronic patient interface unit. The location and orientation of the multielectrode catheter were continuously shown on the workstation during mapping.

Access to the left ventricle was obtained using femoral artery cannulation and the retrograde transaortic approach. The LV was entered by gently passing the partially deployed mini-basket through the aortic valve. The catheter was moved from one region of endocardium to another while the electrograms were recorded continuously from all the electrodes. Cardiac beats were automatically selected by the mapping system

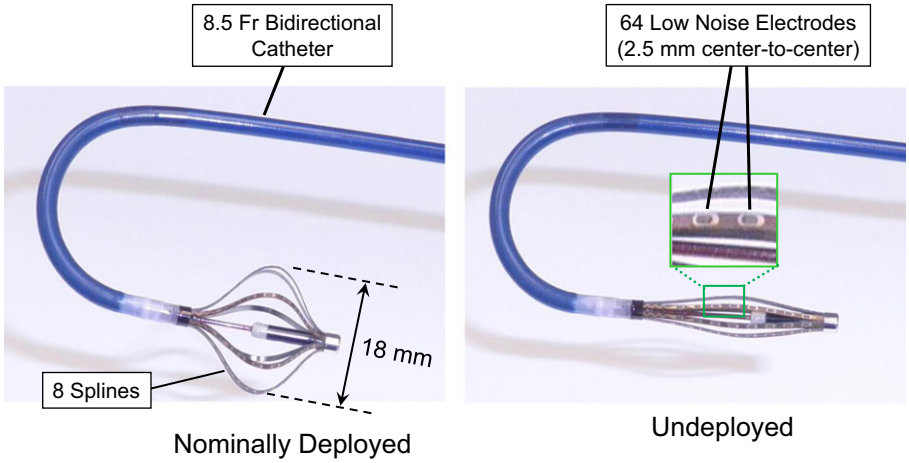

Figure 1. *Mini-basket (64 electrodes) mapping catheter in two states of deployment—nominally deployed (left) and undeployed (right). The mini-basket has eight splines, each with eight tiny, low-noise electrodes (area 0.4 mm^2) separated by 2.5 mm.*

based on cycle length stability, ECG morphology for the beat, electrode location stability, and respiratory gating. If the signals did not satisfy the above criteria, the information was not included in the map. Across all maps, 60% of beats (16,722 of 27,759) were automatically accepted. Multiple electrograms can be acquired from a single beat; each bipole (along each spline of the mapping catheter) can record a bipolar electrogram. The system will automatically delete inner electrogram points as more signals are recorded from spatially outside location. Across all maps, 0.04% of beats (seven of 16,722) were rejected manually, primarily for excess catheter motion. There was only minimal manual editing of the acquired map. The maps were created by including all points recorded within 2 mm from the outermost surface (defined by outermost reach of any of the electrodes in 3D space) of the map. Previously collected points that were now more than 2 mm from the surface as the 3D surface gets defined (during mapping) were automatically excluded from the map. The median mapping time was 54 minutes. Electrogram timing is based on the maximum amplitude of bipolar electrogram. For unipolar electrograms, the maximum dP/dt determines the local activation time at the point. For electrograms with multiple potentials, the system considers the timing of electrograms in the surrounding area to select the correct potential to use for timing. Intracavitary structures such as papillary muscle were not handled differently and could be appreciated as grooves on the 3D geometry shell. Bipolar and unipolar electrograms were filtered at 30–300 Hz and 1–300 Hz, respectively. The voltage for unipolar and bipolar electrograms was derived in the conventional manner, measuring from peak to peak.

The recordings were used to generate an LV activation map, a bipolar voltage map, a unipolar voltage map, and an ILP map, annotating the time and location of the ILPs as described later. The low-voltage area and endocardial scar were defined on the bipolar voltage map as <2 mV and <1 mV, respectively. These values were chosen based on previous animal experiments demonstrating endocardial bipolar voltages in relation to myocardial scar.[12,13]

Manual Validation of Electrograms

The mapping system allows one to review each electrogram point by selecting it. The investigators manually reviewed the recorded electrograms within the low-voltage area (and surrounding 1 cm) to localize the sites exhibiting ILPs. In one map (dog# 4), we validated all of the electrograms in the region of the scar to establish the location and timing of ILPs within the low-voltage areas. The dense contact mapping generated a large number of low-amplitude electrograms (>1,000) in relation to the infarct scars. In the other four dogs, manual annotation was restricted to nonoverlapping points and points separated by 1.5–2 mm due to the large number of electrograms in each scar. Validation consisted of ensuring catheter contact (based on electrogram morphology), annotating the presence or absence of an ILP, and timing of the ILP from the peak of the R wave in ECG lead II. An ILP activation map was created using the timing of the ILP as the activation time. ILPs were defined as discrete (often low amplitude) potentials separated from

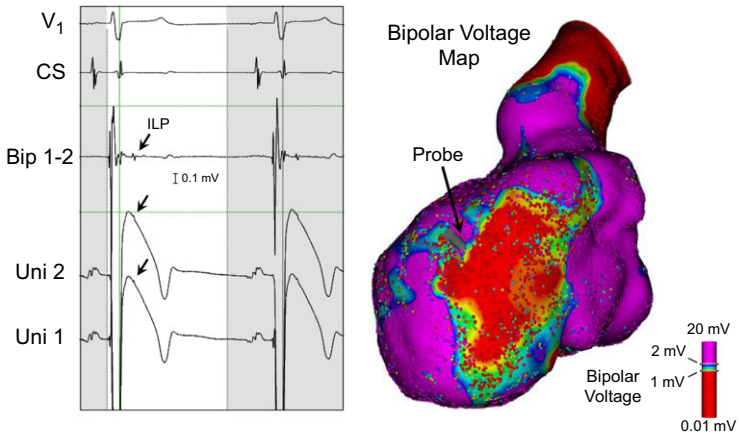

Figure 2. *Example of an isolated late potential (ILP, arrows) and its location on the bipolar voltage map in dog# 4. Left panel: Recordings from the mapping and reference electrodes during sinus rhythm. Traces from the top are electrocardiogram lead V_1, coronary sinus electrogram (CS), and the bipolar (Bip 1–2) and unipolar (Uni 2 and Uni 1) electrograms recorded from mini-basket mapping catheter just inside the anterior border of the scar, at the location depicted by the probe on the bipolar voltage map. The ILP amplitude is 0.07 mV on the bipolar electrogram. Right panel: left ventricular endocardial bipolar voltage map, with voltage represented by color. Red represents bipolar voltage ≤1 mV (scar) and purple represents ≥2 mV (normal). Each dot represents the location of an electrogram recorded within 2 mm of the surface geometry (7,613 electrograms, map resolution 2.6 mm).*

the ventricular potential within the timing of the QRS by an isoelectric interval (Fig. 2). ILPs were required to be consistent between adjacent beats. Potentials thought to be artifacts related to contact with intracardiac structures (such as valve tissue) or catheter rebound at the beginning of LV relaxation were excluded based on the location of the electrode and the timing and morphology of the potential. Total time to review the map, tag the ILPs, and to create the ILP activation map was approximately 2 hours per dog.

For estimating resolution, the 3D surfaces were divided into uniformly distributed triangles (weighted triangulation method), each with an average edge length of 0.6 mm. The distance between each vertex of the triangle and the closest electrogram point was determined. The resolution was estimated as two times the average distance between each triangle vertex and the nearest electrogram point. During review of the map, the system allows the user to move a virtual probe over the geometry to select individual points and display the corresponding electrograms. The electrograms can then be manually annotated to select the activation time of any potential, including an ILP.

Registration of LGE MRI with Electroanatomical Maps

The LGE MRI images were registered with the electroanatomic maps. This was done so that we could select specific areas from the 3D MRI map and the corresponding points from the endocardial voltage map for comparison of voltage to scar type in MRI. The 3D signal intensity maps (LGE maps) generated from the 2D MRI slices as detailed above were aligned and registered with electroanatomic maps using distinct anatomical landmarks (aorta, apex, and papillary muscle grooves) to superimpose the two maps in the Rhythmia Mapping System.

To assess the correlation between electrogram voltages and different MRI scar types, unequivocal areas of each scar type were selected from the LGE MR slices and the corresponding electrogram points from the registered electroanatomical voltage maps were selected for analysis. Up to three sites for each scar type were selected from each MRI and the corresponding electrogram points (10 closest electrograms within 3 mm of each site) were selected from the 3D map.

Statistical Analysis

The unipolar and bipolar electrogram voltages are expressed as median values with interquartile range for each of the tissue types (MRI scar patterns). The significance between the tissue voltage distributions was assessed using the nonparametric Kruskal-Wallis test. The Mann-Whitney test was used to compare voltage (bipolar and unipolar) values between individual tissue types. A second data set with voltage values from the three dogs with large confluent scars (three canine maps) was used for analysis of

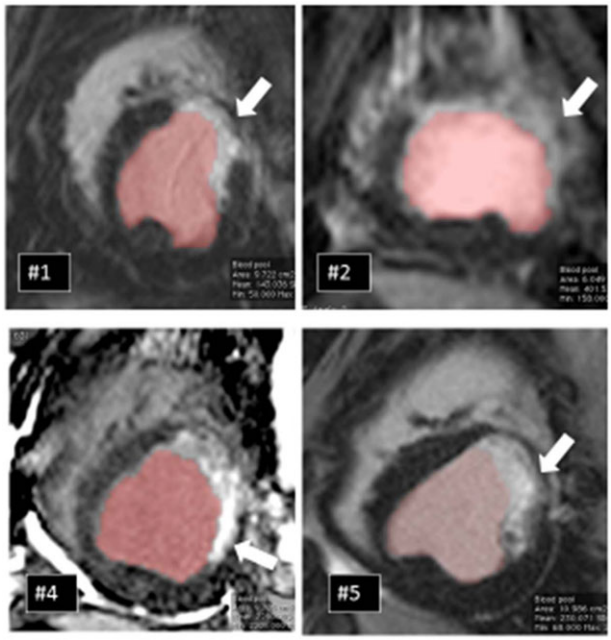

Figure 3. *The scars resulting from the experimental infarcts are shown for dogs# 1, 2, 4, and 5. Dog# 3 had a small infarct and is not shown. The late gadolinium images were used along with T2 magnetic resonance images to define the endocardial border. The scar (white arrows) is identified by late enhancement (white area) adjacent to the blood pool (colored beige).*

the relationship between scar thickness (transmural and nontransmural scars) and endocardial voltages. For comparison of unipolar voltage between transmural and nontransmural scar, an independent *t*-test was used. A probability value <0.05 was considered to be significant.

Results

The LGE MRI images showed late gadolinium enhancement consistent with infarct scar in the anterior and lateral walls of the canine left ventricle. The scar size and thickness varied between animals (Fig. 3). Two dogs had a large, predominantly transmural scar (dogs# 4 and 5); one dog had a large, predominantly endocardial scar (dog# 1); one dog had a small scar (dog# 3); and the remaining dog had a patchy scar (dog# 2).

The electroanatomical maps contained 7,754 $\pm$ 1,960 electrograms per animal, with a mean resolution of 2.8 $\pm$ 0.6 mm. The LV geometry closely approximated the natural geometry of the canine LV and the geometry on cardiac MRI. The area with bipolar voltage <1 mV was 329 and 648 mm^2 in the two dogs with large, predominantly transmural scar, 654 mm^2 in the one dog with a large, predominantly endocardial scar, 325 mm^2 in the dog with a small scar, and 538 mm^2 in the dog with a patchy scar.

The 3D MRI signal intensity maps derived from the gadolinium-enhanced images showed close correlation of scar location and size to the low-voltage areas in the electroanatomical maps. Uniform point sampling from both normal and abnormal voltage (bipolar voltage <2 mV) areas showed matching to gadolinium enhancement in 3D MRI at 87 $\pm$ 7% of the sites for the five dogs. Figure 4 shows the comparison between a confluent scar mapped using the system and the 3D MRI signal intensity map and 2D LGE MRI slices from the same animal. Figure 5 shows the comparison for a patchy scar localized near the LV apex in another dog. The low bipolar voltage area (<2 mV) in the electroanatomical map closely matched the scar on MRI in size and location in all dogs. The dots on the 3D surface reflect the actual position of the recording electrode and the color of the dots represents the electrogram voltage. The surrounding color is dependent on the weighted average of the electrogram voltages in the region. The gradient in voltage between dense scar (red area) and normal myocardium (purple area) represent the scar border and visual comparison showed a close approximation of the scar shape and area to 3D signal intensity map derived from MRI.

Figure 6 shows the distribution of voltages recorded from the endocardium in the areas of different scar types, as defined by MRI, for the five dogs. The bipolar and unipolar voltages from 463 electrograms within scar and 129 electrograms outside of scar were analyzed. The voltage values were significantly different for the different tissues types ($P < 0.01$ by Kruskal-Wallis test). The bipolar voltage from normal tissue was significantly different from all the scar types ($P < 0.01$). Although there was overlap, the distributions of bipolar voltages (Fig. 6A) were significantly different between scar types ($P < 0.01$ for group comparison).

Unipolar voltage was significantly higher for endocardial scar (median 18.6 mV) than dense transmural scar (median 13.6 mV, $P < 0.01$, Fig. 6B). To look for a relationship between unipolar voltage and scar thickness, the unipolar voltage maps were compared with 3D MRI signal intensity maps at 5 mm from the endocardium (midmyocardial to epicardial region) in the three dogs with relatively large scars (dogs# 1, 4, and 5). For this, electrograms from transmural lesions (dense transmural and mottled transmural scar) were compared with electrograms from nontransmural lesions (endocardial and epicardial scar). These samples showed equality of variance for unipolar voltage and showed that unipolar

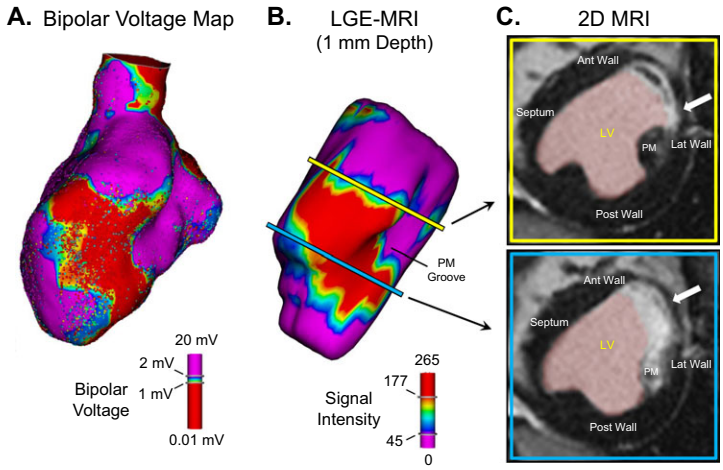

Figure 4. *Comparison of the endocardial bipolar voltage map to the late gadolinium enhancement cardiac MRI (LGE MRI) in dog# 5. (A) Left ventricular endocardial bipolar voltage map showing an anterolateral scar (8,930 electrograms, map resolution 2.7 mm). Red represents bipolar voltages ≤1 mV and purple represents voltages ≥2 mV. (B) 3D reconstructed image (signal intensity map) from the LGE MRI at 1 mm from the blood pool surface (endocardial LGE) showing the large anterolateral scar (red area). Color corresponds to signal intensity, with low intensity in purple and high intensity in red (scar). Note the close correlation between the endocardial low-voltage area (≤1 mV or red area) in panel (A) and the scar (red area) on the LGE MRI signal intensity map at 1-mm depth in panel (B). (C) 2D slices from the LGE MRI corresponding to the locations of the yellow and blue lines in panel (B). The upper (yellow) slice shows endocardial scar (white arrow) extending from the anterior wall to the lateral wall at the margin of the papillary muscle (PM), but sparing the PM. The lower (blue) slice shows a nearly transmural scar extending further posteriorly and involving the PM, also seen on the 3D reconstructed image in panel (B). Ant = anterior; Lat = lateral; PM groove = indented endocardial surface over the papillary muscle; Post = posterior.*

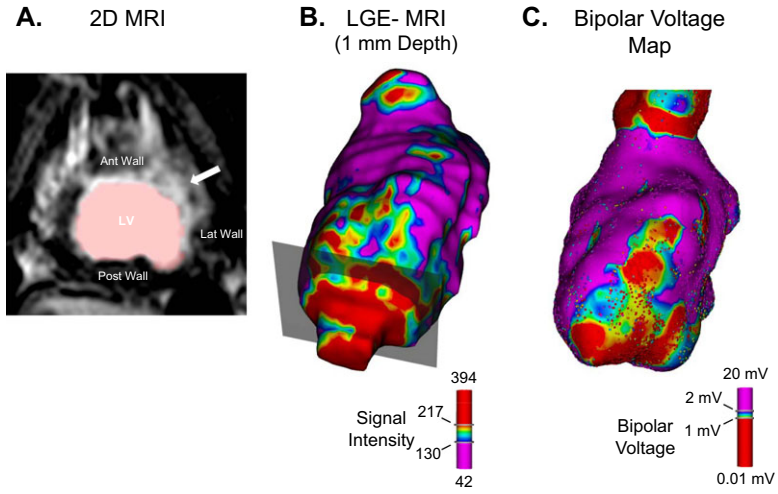

Figure 5. *Comparison of bipolar voltage map to late gadolinium enhancement cardiac MRI (LGE MRI) in dog# 2 with a mottled apical and lateral scar. (A) 2D LGE MRI from the apical region. Note the mottled appearance of the scar (white arrow). Location of the 2D slice is illustrated by the translucent plane in panel (B). (B) 3D reconstructed DE-MRI signal intensity map at 1-mm depth (endocardial LGE) showing the patchy gadolinium enhancement in the apex, anterior, and lateral walls. Color scale represents LGE MRI signal intensity with red areas (high signal intensity) corresponding to scar and purple areas (low signal intensity) corresponding to little or no signal enhancement. (C) Endocardial bipolar voltage map showing patchy areas of low voltage (red areas, ≤1 mV) corresponding to scar in panels (A) and (B). This map contains 9,420 electrograms (map resolution 2.1 mm).*

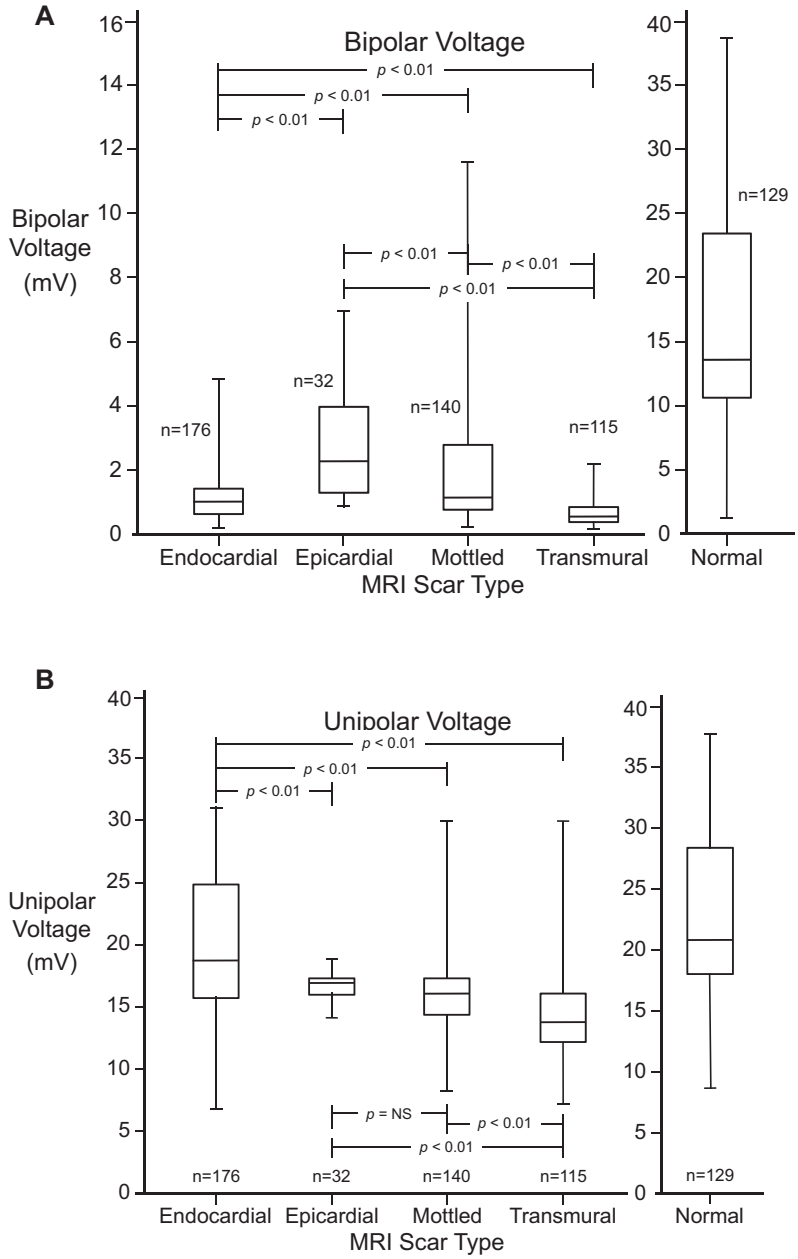

Figure 6. *Relationship between scar type and endocardial bipolar or unipolar voltage. (A) Box plots (median and interquartile range) of endocardial bipolar voltage as function of scar type. (B) Unipolar voltage as a function of scar type. Values of bipolar and unipolar voltage for normal myocardium were significantly greater (P < 0.01) than for each of the four scar types. Significance of differences between groups shown were obtained by the Mann-Whitney test.*

voltage was significantly higher for endocardial scar compared with transmural scar; mean voltage 15.8 ± 2.5 mV versus 13.9 ± 2.3 mV, respectively (P < 0.01). Based on these findings, we compared the unipolar voltage maps, using a low-voltage cutoff of ≤13 mV and a high-voltage cutoff of ≥15 mV, with the MRI signal intensity maps. The unipolar voltage maps appeared to show areas of low voltage corresponding to areas of transmural scar on MRI and delineated transmural scar areas from areas with only endocardial scar (unipolar voltage ≥15 mV and bipolar voltage <1 mV).

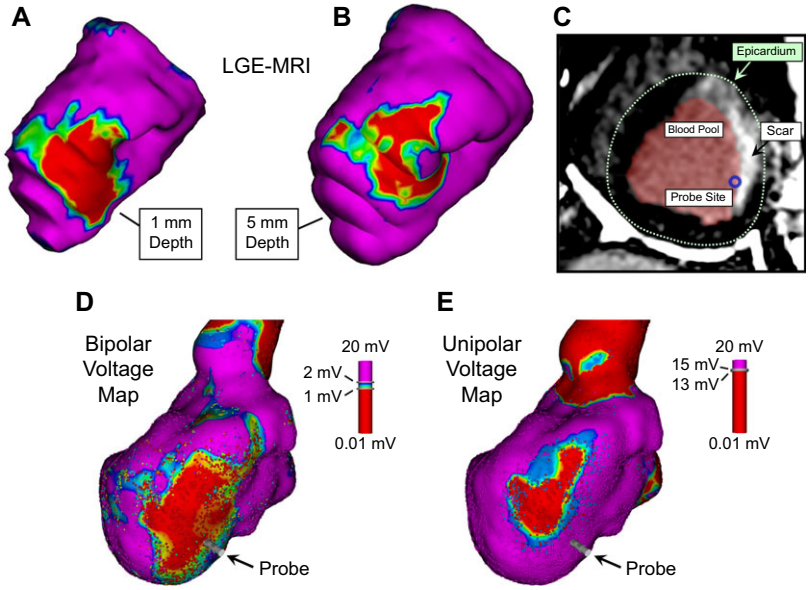

Figure 7. *Correlation of bipolar voltage with endocardial scar and unipolar voltage with epicardial scar in dog# 4. (A) and (B) late gadolinium enhancement cardiac MRI (LGE MRI) reconstructed images at 1 mm and 5 mm from the blood pool surface shows the region of scar (red area) at the endocardial and midmyocardial to epicardial levels, respectively. (C) 2D LGE MRI showing endocardial scar with intact myocardium in the midmyocardial and epicardial layers (thin scar) at the inferolateral region (marked with blue circle), corresponding to the probe location in panels (D) and (E). (D) Bipolar voltage map showing scar (red area, voltage ≤1 mV) in the same location as the scar in the LGE MRI signal intensity map at 1-mm depth (panel A). (E) Unipolar voltage map showing area of voltage ≤15 mV (nonpurple area) which corresponded to the scar in the LGE MRI signal intensity map at 5-mm depth (red area in panel B). Note the red color (bipolar voltage ≤1 mV) at the probe site in panel (D) and purple color (unipolar voltage >15 mV) at the probe site in panel (E). This location had endocardial scar with surviving myocardium above (red color at 1-mm depth DE-MRI in panel (A), purple color in 5-mm depth DE-MRI in panel (B), and corresponds to site marked with a blue circle in 2D MRI in panel C), suggesting thin endocardial scar may be identified using this mapping system by the combination of low bipolar voltage (≤1 mV) and higher unipolar voltage (>15 mV). Probe shown in panels (D) and (E) is a virtual selection tool used during review of the map to select an electrogram from the map*

Figure 7 shows the comparison of the bipolar and unipolar voltage for dog# 4, with the MRI slices for mid-left ventricle and the 3D MRI signal intensity maps. The scars were confluent in only three dogs, and transmural scars also showed heterogeneity between dense and mottled scar.

ILP Maps

The investigators manually examined 1,434 ± 909 electrograms per animal for the presence of ILPs. ILPs were identified in 203 ± 159 electrograms per dog. The ILPs were identified as sharp biphasic or multiphasic potentials separated from the initial ventricular potential early within the QRS complex. In a separate map—called the ILP map, these electrograms containing the ILPs were tagged. The timing of the ILP, measured from the peak of R in ECG lead II, was used to give color annotation to the EGM points in the ILP map (Fig. 8), with earliest ILPs colored red and latest ILPs colored purple. ILPs were localized to MRI scar areas in all animals except one where abnormal electrograms, including low-voltage areas, were observed outside the scar region. Neither scar type nor depth of scar predicted the location of ILPs. The timing of ILPs appeared to show a pattern of spread with early ILPs located in one region of the scar and later ILPs appearing clustered in other regions of the scar. In two dogs with large confluent and predominantly transmural scars, 58% and 89% of ILPs were recorded in regions of transmurality.

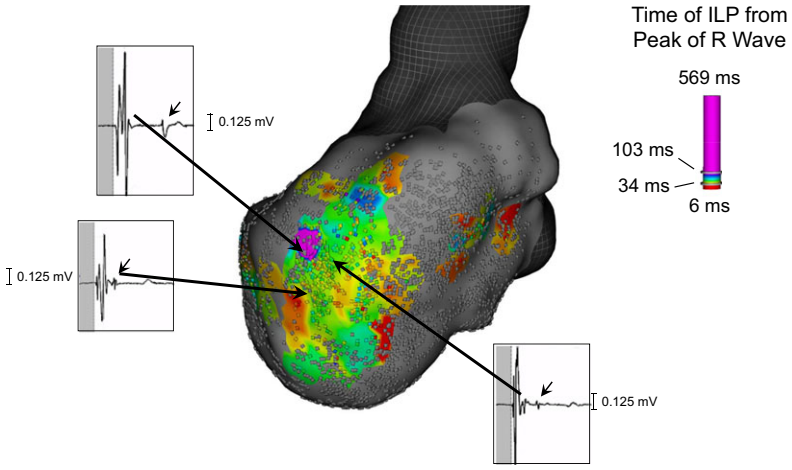

Figure 8. *ILP map in dog# 4 with examples of bipolar electrograms exhibiting an ILP (short arrows). Each colored dot (EGM point) indicates the location of an electrogram containing an ILP. The color scale represents the activation time of the ILP, measured from the peak of the QRS complex (earliest ILPs in red and latest ILPs in purple). Gray dots represent electrograms with no ILP. The background color is interpolated from the color of the EGM points in the map. The timing of the ILP for each of the electrogram was obtained by manual annotation (see text).*

Discussion

This is a demonstration of ultra-high density mapping of infarcted myocardial tissue using this novel mapping system. The mini-basket catheter was easily manipulated into the left ventricle and maneuvered safely throughout the left ventricle in this group of dogs. The geometry generated by the map approximated the shape of the canine LV and the MRI geometry in all five cases. By using a mini-basket (with the shape of a prolate spheroid and 64 electrodes) on a bidirectional catheter, more of the complex endocardial geometry could be mapped. The small, closely spaced electrodes provided high definition contact electrograms with low noise and this helped in identifying late potentials. The system created the surface geometry using the location of the outermost catheter positions and only used electrograms recorded within 2 mm of that constructed surface for activation and voltage maps. Cardiac motion and other related artifacts were excluded by the system using inclusion criteria for electrograms as mentioned in the methods. The accuracy of the geometry and the voltage maps were increased by excluding internal points while the dense mapping ensured high resolution (resolution of 2.8 ± 0.6 mm).

The high-density mapping showed good delineation of scar or abnormal tissue from healthy myocardium as evidenced by the close correlation between the location of low-voltage areas and scar identified on LGE MRI (Figs. 4 and 5). Previous studies had shown that there could be significant areas of nonoverlap between scar visualized in voltage map and MRI,[15] which may be attributed to suboptimal density of electrogram points. The high accuracy was validated by a comparison between electrograms from areas of different scar types that showed that the bipolar voltage recorded from the four scar types were statistically different. While this does not differentiate the different scar types purely based on electrogram voltages, the difference in distribution of voltages attest to the usefulness of high-density mapping.

An attempt was also made to use unipolar voltage maps to differentiate transmural and endocardial areas of scar. The hypothesis was that endocardial areas of scar may show low bipolar voltage but near-normal unipolar voltage. Unipolar voltage maps include the far-field electrical activity from the overlying viable myocardium and hence can differentiate thin endocardial scars from thick transmural scars.[16,17] In this study, in the three dogs with large confluent infarcts, endocardial scar areas showed high unipolar voltage (>15 mV) and transmural scar showed lower unipolar voltage (Fig. 7). High-density mapping improves the utility of unipolar voltage maps by collecting multiple samples from a small region. This may ensure consistent unipolar voltages within each small region and better delineation of voltage gradients across scar types. However, transmural extension of infarction in the animals was relatively patchy and hence the unipolar voltage values derived from this

study may not be applicable in the clinical setting or with another experimental preparation. The unipolar voltage recorded was considerably higher than expected from experience with human scars and other preparations (see section "Study Limitations").

ILPs, which represent delayed activation of surviving muscle bundles within scarred myocardium, are now considered the most suitable targets for ablation of critical isthmuses of the circuits for reentrant tachycardias.[4,6,7,9] In clinical practice, these low-amplitude late potentials are sought in and around low-voltage areas. It has been suggested that ILPs in proximity to heterogeneous MR intensity areas, which may represent relatively preserved myocardium, or ILPs with relatively late timing, are more likely to be critical for sustaining reentry. In dense scar, ILPs typically have very low amplitude and are often missed during point-by-point mapping. In studies published, where they have used multielectrode mapping of relatively large human infarct scars, denser mapping was found to increase the number of ILP targets identified for ablation.[6] In the canine ventricles mapped at high resolution in this study, a large number of ILPs were detected using the new mapping system within the relatively small scars. The small electrodes provided good delineation of these potentials (Fig. 8). A comparison with point-by-point mapping in human ventricle may be necessary to ultimately prove the utility of these high-density maps for ILP delineation and targeting.

Study Limitations

The variation in infarct size between animals and the relatively small area of transmurality compared with total scar area could have affected the outcomes. There were only relatively small areas with purely epicardial scars. The study was performed in canine ventricles, which are smaller than those of humans, and even though ILPs were clearly identified, no data are available regarding the arrhythmogenicity of the substrate in this model. The LGE MRI 3D signal intensity maps were generated from 2D slices with a moderate resolution (6-mm slices). A higher resolution MR imaging system could have produced better 3D MRI models for registration with, and comparison to, the electroanatomical maps. This could have also improved the correlation between voltage and scar type. The tissue to electrogram comparison would also be limited by the presence of partial volume effect and other MRI artefacts as well as the relatively lower resolution of the MRI voxels (1 mm^3). The unipolar voltages recorded from scar tissue were higher than what is expected from experience in human scars, but similar to voltages recorded from canine scars[12] and comparable to values from porcine ventricles.[13] This may have been due to the smaller extent of transmural scar and perhaps due to exclusion of noncontact electrograms as the system automatically excluded electrograms from more than 2 mm from the endocardial surface. Finally, the high-resolution electroanatomical maps were not compared to conventional point-by-point maps using currently available systems. This is required to accurately quantify the utility of unipolar voltage mapping using the tiny electrodes in very high resolution. A comparison between the two for noninfarcted porcine left ventricle has been published.[11] Quantitative histopathological examination was not performed to correlate with the infarct characteristics in MRI and voltage map. Ultimately, human studies are required since chronic infarcts in humans are known to have substantially different scar pathology compared to experimental canine infarcts produced by single coronary ligation.

Conclusions

The high-resolution mapping system and the multielectrode catheter accurately localize ventricular scar and abnormal myocardial tissue in this experimental canine infarct model. The system helps to quickly map and identify abnormal electrograms and delineates the presence, location, and timing of ILPs. Using the high-resolution bipolar and unipolar voltage maps may allow differentiation of scar types and the degree of transmurality.

References

1. Stevenson WG, Wilber DJ, Natale A, Jackman WM, Marchlinski FE, Talbert T, Gonzalez MD, et al. Irrigated radiofrequency catheter ablation guided by electroanatomic mapping for recurrent ventricular tachycardia after myocardial infarction: The multicenter thermocool ventricular tachycardia ablation trial. Circulation 2008; 118:2773–2782.
2. De Bakker JM, Coronel R, Tasseron S, Wilde AA, Opthof T, Janse MJ, van Capelle FJ, et al. Ventricular tachycardia in the infarcted, Langendorff-perfused human heart: Role of the arrangement of surviving cardiac fibers. J Am Coll Cardiol 1990; 15:1594–1607.
3. Arenal A. Tachycardia-related channel in the scar tissue in patients with sustained monomorphic ventricular tachycardias: Influence of the voltage scar definition. Circulation 2004; 110:2568–2574.
4. Bogun F, Good E, Reich S, Elmouchi D, Igic P, Lemola K, Tschopp D, et al. Isolated potentials during sinus rhythm and pace-mapping within scars as guides for ablation of post-infarction ventricular tachycardia. J Am Coll Cardiol 2006; 47:2013–2019.
5. Hsia HH, Lin D, Sauer WH, Callans DJ, Marchlinski FE. Anatomic characterization of endocardial substrate for hemodynamically stable reentrant ventricular tachycardia: Identification of endocardial conducting channels. Heart Rhythm 2006; 3:503–512.

6. Nakahara S, Tung R, Ramirez RJ, Gima J, Wiener I, Mahajan A, Boyle NG, et al. Distribution of late potentials within infarct scars assessed by high-density mapping. Heart Rhythm 2010; 7:1817–1824.
7. Jais P, Maury P, Khairy P, Sacher F, Nault I, Komatsu Y, Hocini M, et al. Elimination of local abnormal ventricular activities: A new end point for substrate modification in patients with scar-related ventricular tachycardia. Circulation 2012; 125:2184–2196.
8. Nakagawa H, Singh D, Beckman KJ, Lockwood D, Po SS, Wu R, Aoyama H, et al. Ablation of unmappable post-MI ventricular tachycardia using substrate mapping during sinus rhythm: Predictors for a recurrence (abstract). Heart Rhythm 2004; 1:S36.
9. Nakagawa H, de Bakker JM, Yokoyama K, Rordorf R, Lazzara R, Jackman WM. Endocardial left ventricular mapping of isolated late potentials within the infarct scar predicts risk of ventricular tachycardia/fibrillation in a canine post-infarction model of sudden death. Circulation 2005; 112:III-661.
10. Nakagawa H, Ikeda A, Sharma T, Lazzara R, Jackman WM. Rapid high resolution electroanatomical mapping: Evaluation of a new system in a canine atrial linear lesion model. Circ Arrhythm Electrophysiol 2012; 5:417–424.
11. Ptaszek LM, Chalhoub F, Perna F, Beinart R, Barrett CD, Danik SB, Heist EK, et al. Rapid acquisition of high-resolution electroanatomical maps using a novel multielectrode mapping system. J Interv Card Electrophysiol 2013; 36:233–242.
12. Gepstein L, Goldin A, Lessick J, Hayam G, Shpun S, Schwartz Y, Hakim G, et al. Electromechanical characterization of chronic myocardial infarction in the canine coronary occlusion model. Circulation 1998; 98:2055–2064.
13. Callans DJ, Ren J-F, Michele J, Marchlinski FE, Dillon SM. Electroanatomic left ventricular mapping in the porcine model of healed anterior myocardial infarction: Correlation with intracardiac echocardiography and pathological analysis. Circulation 1999; 100:1744–1750.
14. Amado LC, Gerber BL, Gupta SN, Rettmann DW, Szarf G, Schock R, Nasir K, et al. Accurate and objective infarct sizing by contrast-enhanced magnetic resonance imaging in a canine myocardial infarction model. J Am Coll Cardiol 2004; 44:2383–2389.
15. Codreanu A, Odille F, Aliot E, Marie PY, Magnin-Poull I, Andronache M, Mandry D, et al. Electroanatomic characterization of post-infarct scars comparison with 3-dimensional myocardial scar reconstruction based on magnetic resonance imaging. J Am Coll Cardiol 2008; 52:839–842.
16. Wolf T, Gepstein L, Dror U, Hayam G, Shofti R, Zaretzky A, Uretzky G, et al. Detailed endocardial mapping accurately predicts the transmural extent of myocardial infarction. J Am Coll Cardiol 2001; 37:1590–1597.
17. Hutchinson MD, Gerstenfeld EP, Desjardins B, Bala R, Riley MP, Garcia FC, Dixit S, et al. Endocardial unipolar voltage mapping to detect epicardial ventricular tachycardia substrate in patients with nonischemic left ventricular cardiomyopathy. Circ Arrhythm Electrophysiol 2011; 4:49–55.